Microstructural Analysis of Activated Carbons Prepared from Paper Mill Sludge by SANS and BET

Kenneth C. Littrell,[‡] Nasrin R. Khalili,*[,†] Marta Campbell,[†] Giselle Sandí,[§] and P. Thiyagarajan[‡]

Department of Chemical and Environmental Engineering, Illinois Institute of Technology, Chicago, Illinois 60616, and Intense Pulsed Neutron Source and Chemistry Divisions, Argonne National Laboratory, 9700 South Cass Avenue, Argonne, Illinois 60439

Received July 9, 2001. Revised Manuscript Received October 5, 2001

Small-angle neutron scattering (SANS) and N_2-BET analysis were used to characterize the microstructure of a series of activated carbons produced from paper mill sludge using $ZnCl_2$. N_2-BET and SANS data indicate that the micro- and mesoporous surface areas of the carbons increase with the concentration of $ZnCl_2$ used in their preparation. Contrast variation SANS studies demonstrate the existence of two different phases, a zinc-rich particle phase and a bulk carbon phase with nanopores. Both phases are largely accessible to the solvent. The size and morphology of the pores and inclusions were determined from the SANS data. The pores are found to be roughly rodlike. The radii and volumes of the pores increase with increasing the amount of activating agent ($ZnCl_2$) used for the production of the carbons. On the basis of SANS results, we propose a conceptual model describing structural characteristics of the produced carbons.

1. Introduction

Activated carbons play an important role in many areas of modern science and technology such as purification of liquids and gases, separation of mixtures, and catalysis. Their value in any particular application is determined by the characteristics of their surface structure.[1−3] The method of preparation including the characteristics of the raw starting material, activation agents, activating process, etc., can strongly influence the microstructure of the carbons and hence their function.

One of the key steps in the production of activated carbons is chemical activation through the impregnation of the raw material with chemicals such as phosphoric acid,[4] potassium hydroxide,[5] or $ZnCl_2$.[6−8] These additives are known to enhance carbonization, resulting in improved development of the pore structure.[9] The presence of a significant amount of micropores (according to IUPAC system, pores with widths <20 Å are classified as micropores, those with widths between 20 and 500 Å as mesopores, and those with widths >500 Å as macropores) and a high surface area are necessary for a carbon to function as a highly adsorptive medium, particularly, in gas phase purification processes. These types of carbons typically contain pores with effective radii considerably smaller than 16−20 Å.[10] However, activated carbons with well-developed transitional porosity and pore diameters between 20 and 500 Å have found their application in the treatment of liquid phase systems such as wastewater and water containing coloring impurities.[11]

Although a relatively wide range of porous solid adsorbents for a given industrial application can be obtained solely through chemical activation processes, physical activation can also be used to further enhance adsorbent pore structure by partial oxidation of the carbonized material.[12−14] Among the activating agents used for the production of activated carbon from carbonaceous material, $ZnCl_2$ has been proven to be one of the most effective impregnants.[9,15] According to Caturla et al.,[9] $ZnCl_2$ acts as a dehydrating agent, influencing the decomposition of carbonaceous material during the pyrolysis, thus restricting the formation of tar and

* To whom correspondence should be addressed. Tel: (312) 567−3534. Fax: (312) 567−8874. E-mail: khalili@iit.edu.
† Illinois Institute of Technology.
‡ Intense Pulsed Neutron Source Division, Argonne National Laboratory.
§ Chemistry Division, Argonne National Laboratory.

(1) Boehm, P. H. *Adv. Catal.* **1996**, *16*, 197.
(2) Bansal, R. C.; Donnet, J.; Stoeckli, F. *Active Carbon*; Marcel Dekker Inc.: New York, 1988; p 26.
(3) Kinoshita, K. *Carbon: Electrochemical and Physiochemical Properties*; John Wiley and Sons: New York City, NY, 1988; p 200.
(4) Molina-Sabio, M.; Rodriguez-Reinoso, F.; Caturla, F.; Selles, M. J. *Carbon* **1995**, *33* (8), 1105.
(5) Otowa, T.; Nojima, Y.; Miyazaki, T. *Carbon* **1997**, *35* (9), 1315.
(6) Ibarra, J. V.; Moliner, R.; Palacios, J. M. *Fuel* **1991**, *70*, 727.
(7) Hourieh, M. A.; Alaya, M. N.; Youssef, A. M. *Adsorpt. Sci. Technol.* **1997**, *15* (6).
(8) El-Nabarawy, T. H.; Mostafa, M. R.; Youssef, A. M. *Adsorpt. Sci. Technol.* **1997**, *15* (1), 61.
(9) Caturla, F.; Molina-Sabio, M.; Rodriguez-Reinoso, F. *Carbon* **1991**, *29* (7), 999.
(10) Boppart, S.; Ingle, L.; Potwora, R. J.; Rester, D. O. *Chem. Process.* **1996**, 79.
(11) Walker, P. L. *Chemistry and Physics of Carbon*; Marcel Dekker: New York, 1996.
(12) Torregrosa-Macia, R.; Martin-Martinez, J. M.; Mittelmeijer-Hazeleger, M. C. *Carbon* **1997**, *35* (4), 447.
(13) Molina-Sabio, M.; Gonzalez, M. T.; Rodriguez-Reinoso, A.; Sepulveda-Escribano, A. *Carbon* **1996**, *34* (4), 505.
(14) Rodriguez-Reinoso, F.; Molina-Sabio, M.; Gonzalez, M. T. *Carbon* **1995**, *33* (1), 15.
(15) Balci, S.; Dogu, T.; Yücel, H.; *J. Chem. Technol. Biotechnol.* **1994**, *60*, 419.

10.1021/cm010653u CCC: $22.00
Published on Web 11/30/2001

increasing the carbon yield. The degradation of cellulose material and the aromatization of the carbon skeleton upon $ZnCl_2$ treatment result in the creation of the pore structure. These pores are the interstices left vacant upon the removal of $ZnCl_2$ from the carbon matrix by intensive washing.[9,13,15,16] These studies have clearly demonstrated that the amount of $ZnCl_2$ used during chemical activation significantly impacts the structural characteristics of the carbons.

While most industrial-grade carbons are made from bituminous coal, any carbonaceous material can be converted into activated carbon. The practicality and environmental advantages of using waste materials such as coconut shells, bones, wood, coal, petroleum coke, lignin, lignite, biosolids, etc., as raw materials for the production of activated carbons has been recently investigated.[17−20,24] Regardless of the source of raw material or the preparation technique, activated carbons must include structural characteristics necessary for their application as adsorbents or catalysts. Structural information about the carbons in terms of surface area, pore size, and pore volume determines their selection for a given application. Although BET[1,3,11] has been traditionally used to characterize the surface area of carbons by using Dubinin−Radushkevich (DR) and α_s plots, it does not provide direct information on the exact structure and morphology of the pores in the carbons. Small-angle neutron scattering (SANS) is a versatile technique for the characterization of the microstructure of porous solid materials, and it has the highest sensitivity in the length scales of 1−100 nm.[25−28] Since SANS arises from the presence of inhomogeneities in the neutron scattering length density in a system, it can be used to obtain information on the size, structure, and geometric arrangement of pores in solids as well as the accessibility to solvents. The particles and pores defining the structure of an activated carbon can produce strong scattering, depending on their organization.

In this paper, we present results on the relationship between the preparation and structure for a series of activated carbons produced from paper mill sludge upon chemical activation by various amounts of $ZnCl_2$. A N_2-BET test was used to characterize the nature of the porosity within the carbon structure. The SANS data, however, was used to study the structure and morphology of the pores, surface-to-volume ratios of the pore network, and the accessibility to the solvents across a broad range of length scales. Due to the importance of the accessibility of solvents to the pores of these activated carbons in real systems, a contrast variation SANS study, where the sample is placed in contact with a series of chemically identical solvents with differing neutron scattering length densities, was carried out on one of the carbons.

2. Experimental Methods

A series of activated carbons identified as Zn_xC, where x is the mass ratio of the $ZnCl_2$ to the dried sludge and ranges from 0.75 to 2.5, were prepared from paper mill sludge. The raw paper mill sludge was dried in an oven at 110 °C for 24 h and crushed mechanically by using a paint mixer. The crushing produced smaller particles that increased the surface area thus enabling more efficient chemical activation of the raw material. The samples were sieved after mechanical crushing to obtain particles with sizes smaller than 600 μm to be suitable for the chemical activation process. The samples were chemically activated by using five different mass ratios of $ZnCl_2$ to dried sludge: 0.75, 1.0, 1.5, 2.0, and 2.5.[20] To ensure a complete reaction between $ZnCl_2$ and sludge particles, the sludge was mixed with $ZnCl_2$ at 85 °C for 7 h.

After chemical activation, samples were dried in air at 110°C for 24−36 h. The time required for drying varied depending on the amount of $ZnCl_2$ used for the activation process, with higher impregnation ratios requiring longer drying times. After drying, the sludge was again crushed into a fine powder. The chemically activated samples were exposed to light and humidity for about 22 h to enhance the development of the pore structure during pyrolysis.[20] Pyrolysis of the samples was carried out in an inert environment (70 mL min^{-1} flow of nitrogen gas) at 800 °C for 2 h. Upon completion of the pyrolysis, the sample was crushed by using a mortar and a pestle, then treated with 500 mL of 1.2 M HCl, and followed by washing with 500 mL of distilled water to remove excess $ZnCl_2$ and residual inorganic matter. After drying in air, the samples were transferred to 20 mL vials for storage prior to conducting the physical activation process. During the physical activation, the samples were heated for 2 h at 800 °C in a mixture of 75% CO and 25% CO_2. Upon completion of the physical activation, the carbons were characterized by BET.

The SANS measurements were performed at the SAND, the time-of-flight SANS instrument at the Intense Pulsed Neutron Source at Argonne National Laboratory, using cylindrical Suprasil sample containers with a path length of 1 mm. For strongly scattering samples such as these, SAND provides high-quality data in a Q (scattering momentum-transfer vector length) range of 0.0035−0.8 $Å^{-1}$ in a single measurement. The carbon samples were ground into a powder for the SANS measurements. The cells were filled with equal weights of the dry powders and packed using the three-tap method[25] to ensure that the sample densities were nearly equal. Samples with $ZnCl_2$/paper mill sludge ratios of 1, 1.5, 2, and 2.5 were studied as dry powders. In addition, a contrast variation SANS study was performed on a $Zn_{2.5}C$ sample by preparing the powdered sample of known weight as slurries in a series of mixtures of normal and fully deuterated toluene, with deuterated toluene proportions of 0, 25, 50, 75, and 100%. In preparing the slurries, the powder was slowly evacuated to avoid the formation of air bubbles while adding the solvent. The scattering from an identical empty cell was used for background correction in these measurements. The incoherent scattering from the solvents was fitted and subtracted during the analysis of the SANS data.

3. Results and Discussion

3.1. N_2-BET Adsorption Isotherm Data. The N_2 adsorption isotherm data for the activated carbons are presented in Figure 1. Analysis of the isotherm data (Table 1) by using the DR equation, α_s, Barret−Joyner−

(16) Ahmadpour, A.; Do, D. D. *Carbon* **1997**, *35* (12), 1723.
(17) Kruk, M.; Jaroniec, M.; Gadkaree, K. P. *Colloid Interface Sci.* **1997**, *192*, 250.
(18) Dai, X.; Antal, M. J., Jr. Proc. Am. Chem. Soc. Natl. Meet. 1997, *42* (3), 864.
(19) Lopez-Ramon; Moreno-Castilla, C.; Rivera-Utrilla, J.; Hidalgo-Alvarez, R. *Carbon* **1993**, *31*, 815.
(20) Khalili, N. R.; Arastoopour, H.; Wolhof, L. K. *Synthesizing Carbon from Sludge.* U.S. Patent 6,030,922, 2000.
(21) Walhof, L. K. M.S. Thesis, Illinois Institute of Technology, Chicago, IL, 1998.
(22) Jeyaseelan, S.; Lu, G. Q. *Water Sci. Technol.* **1996**, *34* (3−4), 499.
(23) Lu, G. Q.; Do, D. D. *Carbon* **1991**, *29* (2), 207.
(24) Martin, M.; Balagure, M. D.; Rigola, M. Proceedings, Beneficial Reuse of Water and Biosolids Conference, Marbella, Malaga, Spain, April 6−9, 1997; pp 9−41.
(25) Sandí, G.; Thiyagarajan, P.; Carrado, K. A.; Winans, R. A. *Chem. Mater.* **1999**, *11*, 235.
(26) Beaucage, G.; Aubert, J. H.; Lagasse, R. R.; Schaefer, D. W.; Rieker, T. P.; Erlich, P.; Stein, R. S.; Kulkarni, S.; Whaley, P. D. *J. Polym. Sci., Part B: Polym. Phys.* **1996**, *34*, 3063.
(27) Beaucage, G. *J. Appl. Crystallogr.* **1996**, *29*, 134.
(28) Beaucage, G. *J. Appl. Crystallogr.* **1995**, *28*, 717.

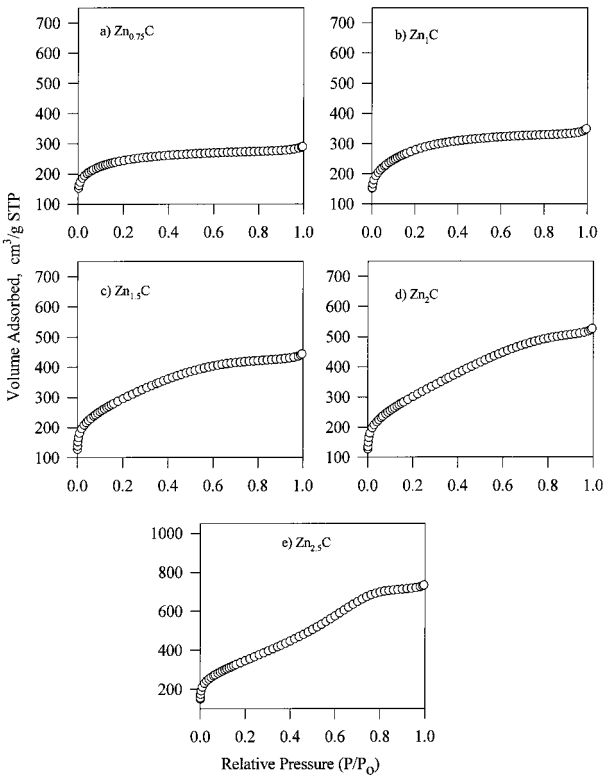

Figure 1. N_2 adsorption isotherms obtained for the produced activated carbons by using $ZnCl_2$/sludge ratios of (a) 0.75, (b) 1, (c) 1.5, (d) 2, (e) 2.5, and (f) 3.5.

Halenda (BJH) method, and micropore analysis (MP) method[1,3,11,29,30] together suggests a systematic dependence of the development of micro- and mesoporosity on the degree of chemical activation. As shown, the mesopore volume of the carbons approximately doubled as the amount of $ZnCl_2$ used for chemical activation of raw material increased from 1.0 to 2.5 in terms of $ZnCl_2$/sludge mass ratio. Figure 2 illustrates the change in the shape of the adsorption−desorption isotherms at two $ZnCl_2$/sludge ratios. Together, these trends show the strong dependence of the pore network structure on the method of preparation. The estimated surface area and micropore volume show a similar trend. The pore diameter for the carbons $Zn_{0.75}C$ and Zn_1C is smaller than 20 Å, while the activated carbons produced with a $ZnCl_2$/sludge ratio up to 2.5 contain a fairly narrow mesoporous structure (≥30 Å). The percentage of the total pore volume occupied by the micropores is an inverse function of the estimated pore size. The calculated micropore volumes indicate that increase in the amount of $ZnCl_2$ not only enhances microporosity but also promotes the formation of mesoporous structure.

The agreement between the estimated micropore volumes from the DR equation and α_s plots varies depending on the degree of impregnation (the micropore volumes estimated from the DR and α_s methods are comparable for carbons activated with a low amount of $ZnCl_2$ ($x < 1.5$), but the α_s micropore volume was found to be higher than that estimated from the DR method for carbons produced with $x > 1.5$ (0.990 vs 0.486 cm^3 g^{-1} calculated from the DR equation). These data suggest that α_s micropore volumes include the volume of the small mesopores in the total micropore volume while DR micropore volumes are a measure of the volume of micropores only.

Although the analysis of the N_2 adsorption data indicates a significant impact of the method of production on the microscopic structure of the carbons studied, this analysis does not provide the direct information on pore size and morphology that is essential to predict the behavior of the carbons for a given application. Therefore, SANS was used to obtain the information on the structure and morphology of the pores and their accessibility to solvents.

3.2. SANS Data. The SANS data were initially analyzed by using a version of the unified Guinier-power law fitting procedure described by Beaucage.[26−28] This model describes a wide range of data with multiple levels of structures by using a single mathematical model and has proven useful in studies of a variety of systems ranging from polymer blends to silicates with hierarchical structures. In our implementation, the scattering from the sample is described as the sum of the scattering from two levels of structural organization, with the scattering from each level given by

$$I_i(Q) = A_i \exp\left(-\frac{Q^2R_{Gi}^2}{3}\right) + (Q_i^* L_i)^{-D_i} \qquad (1)$$

where $I_i(Q)$ is the scattering intensity, A_i is the intensity of the scattering from that level of structure extrapolated to $Q = 0$ Å^{-1}, R_{Gi} is the radius of gyration describing the maximum extent of that level, D_i is the power law exponent, L_i is the characteristic length scale, and Q_i^* is the function of Q scaled to cut off the power law scattering of that structural level on length scales larger than R_{Gi}.[27,28] The scattering from the first, low-Q structural level is multiplied by [exp(− $Q^2R_{G2}^2/3$)], the Guinier law for the second structural level, decoupling the scattering between the two levels and causing the first level to act as a structure factor.

As Figure 3 illustrates, this function describes the data well over the full range of Q measured. Since the data showed no evidence of leveling off at low Q, we arbitrarily fixed the radius of gyration of the first structural level at 1 μm and suppressed its Guinier region scattering by setting $A_1 = 0$. We point out that the 1 μm size that was assumed for the first structural level will not affect the structural parameters obtained from the scattering data at $Q > 0.01$ Å^{-1} that results from the pores produced by $ZnCl_2$. Table 2 shows the results of these fits, which indicate that the scattering from the dry powder samples in the low-Q region ($Q <$ 0.01 Å^{-1}) follows a power law with exponents between −3 and −4, resembling the scattering from coals. This power law scattering may be either due to large objects with fractal (rough) surfaces or from a polydisperse collection of spherical objects.

Since the low-Q power law scattering is similar for all the powder samples, we subtracted the fitted low-Q power law scattering from the data for all the powder samples to emphasize the scattering from the nanometer-scale pores as illustrated in Figure 4. In Figure 5

(29) Campbell, M. M.S. Thesis, Illinois Institute of Technology, Chicago, IL, 1999.
(30) Sing, K. S. W.; Everett, D. H.; Haul, R. A. W.; Moscou, L.; Pierotti, R. A.; Rouquerol, J.; Siemieniewska, T. *Pure Appl. Chem.* **1985**, *57* (4), 603.

Table 1. Effect of Chemical Activation on Surface Physical Properties of the Carbons Produced from Paper Mill Sludge

impregnation ratio	$V_{(0)DR}$[a] ($cm^3\ g^{-1}$)	V_{total}[b] ($cm^3\ g^{-1}$)	micropore vol (%)	estimated pore size (Å)	$V_{(0)\alpha_s}$[c] ($cm^3\ g^{-1}$)	avg diam* (Å)	total surface area ($m^2\ g^{-1}$)
$Zn_{0.75}C$	0.361	0.446	81	<20	0.400	19.93	895
Zn_1C	0.377	0.534	71	<20	0.485	21.06	1015
$Zn_{1.5}C$	0.393	0.679	58	25	0.595	25.46	1067
Zn_2C	0.398	0.809	59	30	0.657	29.62	1095
$Zn_{2.5}C$	0.486	1.128	43	30	0.990	36.13	1249

[a] $V_{(0)DR}$ = micropore volume estimated from DR equation. [b] V_{total} = total pore volume. [c] $V_{(0)\alpha_s}$ = micropore volume estimated using α_s method.

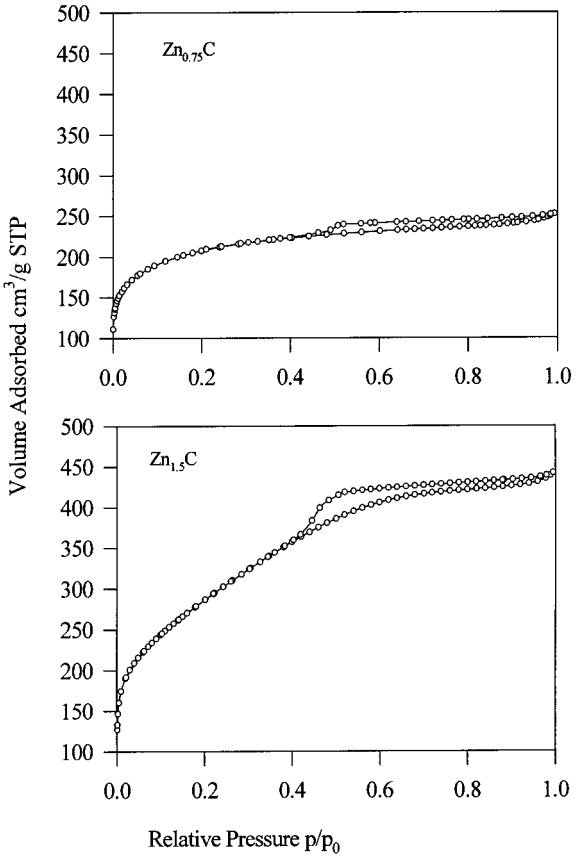

Figure 2. Representative N_2 adsorption−desorption isotherms for carbons produced with different $ZnCl_2$/sludge ratios.

we show the data for the scattering from the pores for the powder samples. Note that the subtraction of the low-Q power law from the scattering data does not affect the shape of the curve in the region above $Q = 0.02$ Å^{-1}. It is clear from Figure 5 that the scattering at $Q > 0.02$ Å^{-1} increases as the $ZnCl_2$ concentration, used in the preparation of the carbons, increases. The knee (the point at which the scattering intensity begins to level off as Q decreases) also occurs at progressively lower values of Q as the $ZnCl_2$ concentration increases, indicating the presence of progressively larger structural elements in the carbons. Similar trends can be seen from the radius of gyration and the $I(0)$ values given in Table 2. These trends are consistent with the increases seen in the specific volumes, specific surface areas, average pore radii and volumes, and proportions of larger pores in the BET results as the proportion of zinc, used in activation, is increased.

The morphology of the pores in these carbons was studied by using the modified Guinier plot for rodlike objects, a plot of $QI(Q)$ vs Q^2, shown in Figure 6. The clear presence of the linear region at low Q in Figure 6

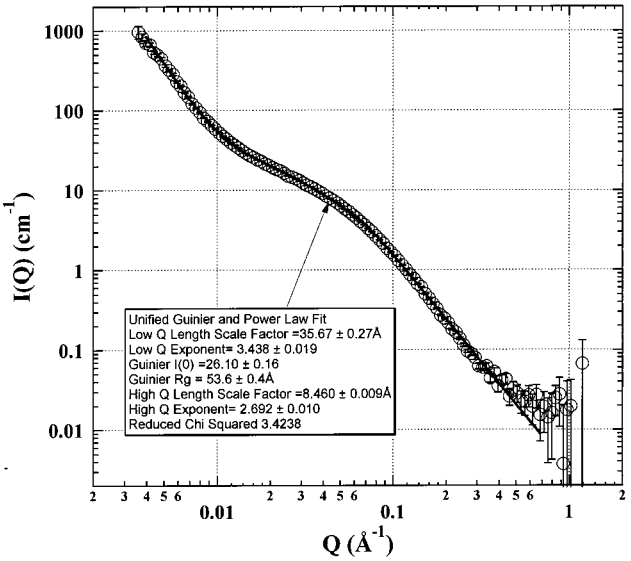

Figure 3. Comparison of the unified fit function to the SANS data for the dry powder sample prepared with a $ZnCl_2$/sludge ratio of 2.5. The other fits are similar in quality.

indicates that the pores in these carbons are elongated. The slope of this linear region at $Qr \leq (2)^{1/2}$ is $-r^2/4$, where r is the average cross-sectional radius of the pores. As Figure 6 shows, the average pore radius increases with increasing $ZnCl_2$ concentration. The data with the low-Q power law subtracted from it was used in this analysis. The average length of a rodlike pore can be calculated from cross-sectional radius and the radius of gyration by using the relation

$$l = (12(R_G^2 - r^2/2))^{1/2} \qquad (2)$$

The cross-sectional radii and lengths of the pores are given in Table 2. It is likely that these lengths represent a persistence length—the length over which the pores can be thought of as nearly straight—instead of the overall length of the pores.

One of the advantages of SANS is that the contrast between a sample and its environment or different parts of a sample can be readily varied by isotopic substitution of hydrogen with deuterium, due to the large difference between the scattering lengths of hydrogen and deuterium. We have used this approach to study the pore accessibility of these carbons through a solvent contrast variation study performed by using slurries of the sample, with a $ZnCl_2$ ratio of 2.5, immersed in different mixtures of toluene (scattering length density $= 0.939 \times 10^{10}$ cm^{-2}) and deuterated toluene (scattering length density $= 5.64 \times 10^{10}$ cm^{-2}). Toluene was selected as the solvent as it has been found to wet these carbons well.

Table 2. Relevant Parameters Obtained from the SANS Data for the Dry Powder Samples

$ZnCl_2$/sludge ratio	low-Q power law exponent	Guinier $I(0)$ intensity (cm^{-1})	radius of gyration (Å)	cross-sectional radius (Å)	length (Å)
1:1	3.193(9)	2.63(8)	30.6(13)	7.74(24)	104(10)
1.5:1	3.518(11)	4.16(6)	33.9(7)	10.66(17)	114.5(12)
2:1	3.624(12)	6.98(5)	39.9(4)	13.38(16)	134.3(4)
2.5:1	3.438(19)	26.10(16)	53.6(4)	20.52(17)	178.7(3)

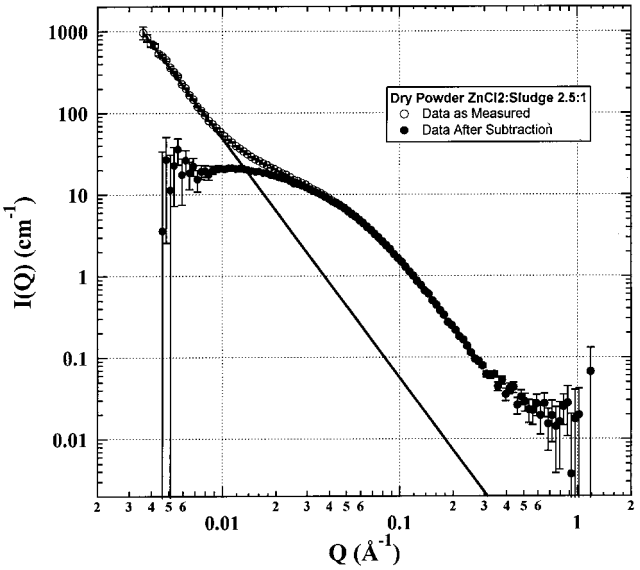

Figure 4. Demonstration of the subtraction of the low-Q power law scattering to emphasize the scattering from the newly formed porosity.

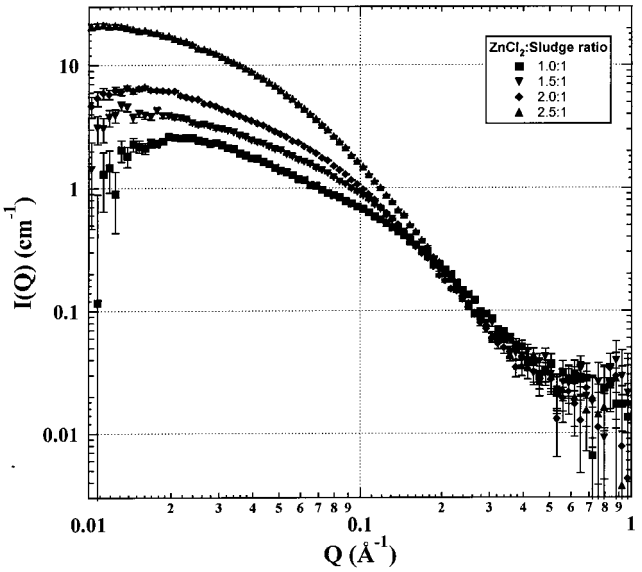

Figure 5. SANS data of the carbon powders after the subtraction of the power law scattering from the low-Q region. The scattering intensity increases with increasing $ZnCl_2$ concentration, indicating the monotonic growth of the pore size with increasing Zn during the preparation.

The scattering data for the carbon slurries were also fitted by using the two-layer unified fit model described above with the first-layer power law exponent fixed to −3.44, the value obtained for the dry powder of this sample. This is a reasonable approach as toluene does not cause these carbons to swell and hence should not change the form of the observed scattering function at the small Q values corresponding to length scales much larger than the effective diameter of the toluene molecules. A constant background term was included as a fit parameter to account for the incoherent scattering from the hydrogen and deuterium atoms in the solvent. The results from the fits are presented in Table 3.

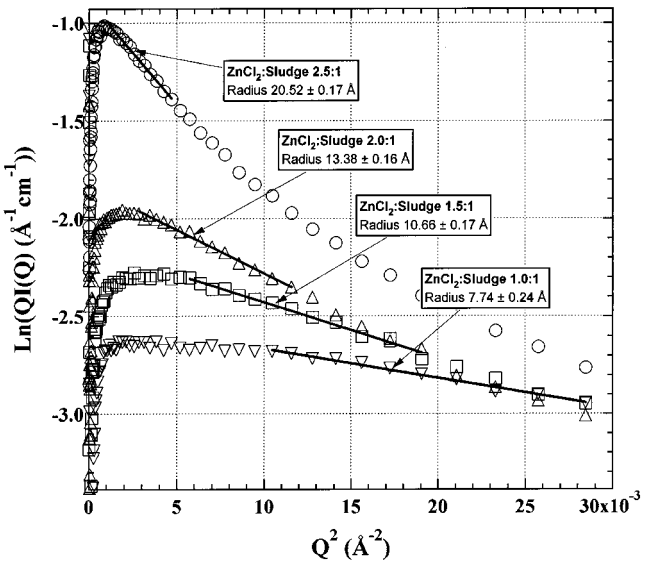

Figure 6. Modified Guinier plot for rodlike forms for the powder data. The data suggest the presence of tubular pores with average radii that increase as the amount of $ZnCl_2$, used to produce the carbon, increases.

The adjusted data for the low-Q power law and the constant background is presented in Figure 7. As shown, the behavior of these samples in the contrast variation study is much more complicated than that expected for a homogeneous system, for which the coherent scattering intensity will vary uniformly at all Q values as the deuteration of the solvent (contrast) is varied. Instead, for the carbons, the coherent scattering intensity varies differently in the regions of Q that correspond to different length scales. At low Q (region I of Figure 7), the coherent scattering intensity becomes low at an intermediate level of deuteration of the toluene, indicating that most of the scattering from the longer length scales arises from structures with a scattering length density different from that of bulk carbon (see below). The fit to the scattering data at $Q = 0.01$ $Å^{-1}$ to a parabola in Figure 8 indicates that the scattering from the larger objects reaches a minimum when the scattering length density of the solvent is 3.774×10^{10} cm^{-2}. Since it is possible that even after processing some Zn may remain in the sample in the form of $ZnCl_2$ (scattering length density $= 3.19 \times 10^{10}$ cm^{-2}), ZnO (4.76×10^{10} cm^{-2}), or metallic zinc (3.73×10^{10} cm^{-2}), we interpret this to indicate the prevalence of particles of a Zn-rich phase.

Interestingly, at high-Q region (III in Figure 7), the range corresponding to smaller inhomogeneities in the coherent scattering intensity varies differently than that observed at region I corresponding to larger inhomoge-

Table 3. Relevant Parameters Obtained from the Contrast Variation SANS Studies of the Carbon Sample Prepared by Using the $ZnCl_2$/Sludge Ratio of 2.5:1

solvent scattering length density (10^{10} cm^{-2})	Guinier $I(0)$ intensity (cm^{-1})	radius of gyration (Å)	intensity at Q = 0.01 Å^{-1} (cm^{-1})	intensity at Q = 0.1 Å^{-1} (cm^{-1})	incoherent background (cm^{-1})
0.939	15.18(23)	51.5(10)	33.0(8)	1.128(17)	0.185(3)
2.11	6.50(10)	40.9(9)	15.0(5)	0.653(13)	0.171(4)
3.29	4.22(6)	69.5(17)	6.3(4)	0.371(10)	0.1147(29)
4.46	3.77(11)	65.1(15)	7.2(4)	0.169(8)	0.0803(27)
5.64	8.42(11)	67.2(5)	17.2(4)	0.078(5)	0.0357(14)

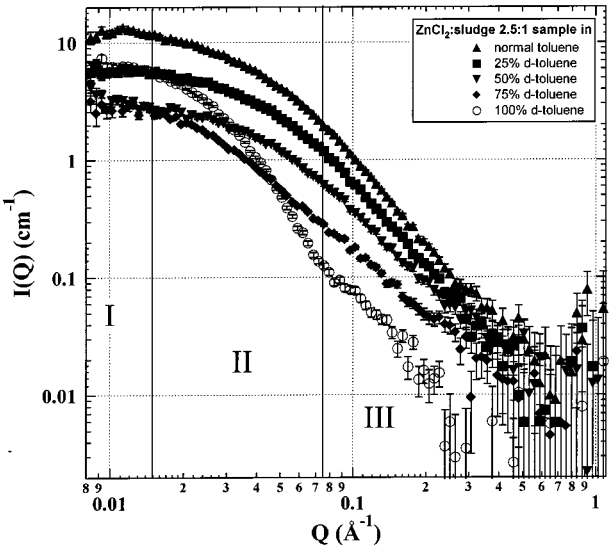

Figure 7. Contrast variation SANS data with the fitted low-Q power law scattering and incoherent background subtracted showing the presence of two different kinds of scattering objects.

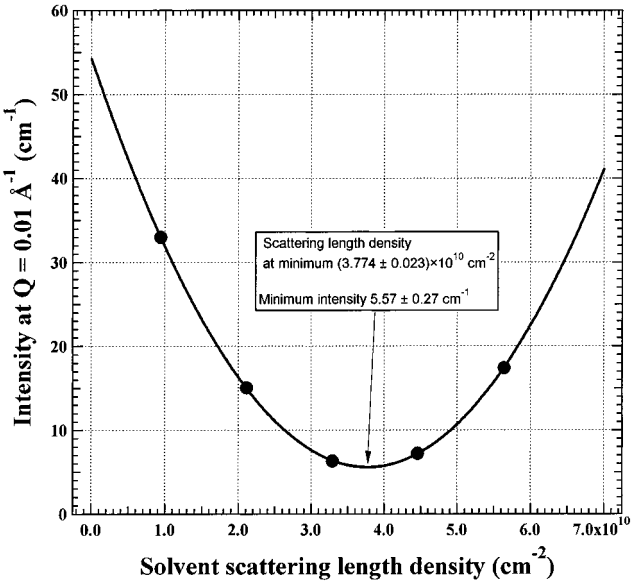

Figure 8. Coherent scattering at $Q = 0.01$ Å^{-1} from the $Zn_{2.5}C$ sample as a function of solvent scattering length density. The minimum occurs at a scattering length density of 3.774×10^{10} cm^{-2}, suggesting the presence of Zn-rich particles.

neities as the deuteration level of toluene is varied. The scattering intensity is large at $Q = 0.1$ Å^{-1} for samples in normal toluene, and it monotonically decreases as the deuteration level of the solvent increases, attaining a minimum value in the 100% deuterated toluene. The coherent scattering intensities at $Q = 0.1$ Å^{-1} were plotted as a function of the scattering length density of the solvent and fitted to a parabola as shown in Figure 9. It is clear from Figure 9 that the coherent scattering intensity from the smaller inhomogeities becomes a minimum when the scattering length density of the solvent is 5.92×10^{10} cm^{-2}, close to the scattering length density of bulk amorphous carbon. Based on these results, we believe that the scattering in the high-Q region arises from the pores in the bulk amorphous carbon.

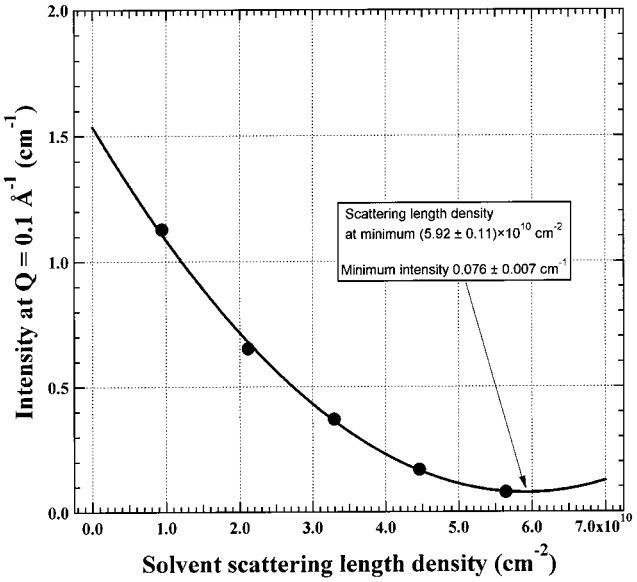

Figure 9. Coherent scattering at $Q = 0.1$ Å^{-1} from the $Zn_{2.5}C$ sample as a function of solvent scattering length density. The minimum occurs at a scattering length density of 5.92×10^{10} cm^{-2}, compatible with the scattering length density of bulk amorphous carbon.

It is interesting to note that during contrast variation the minima in the coherent scattering intensities at both low Q (0.01 Å^{-1}) and high Q (0.1 Å^{-1}) become about 10% or less of the scattering intensity values at respective Q values for the $Zn_{2.5}C$ powder. This demonstrates that both the pores and the surfaces of the particles of the Zn-rich phase must be accessible to the solvent, as the scattering intensity would not have varied to the extent observed here otherwise.

4. Conclusions

N_2 adsorption isotherm data obtained for a series of activated carbons produced from paper mill sludge showed that increasing amount of $ZnCl_2$ enhances the total micropore volume and causes the formation of a higher proportion of larger micropores in the carbon structure. The detailed surface analyses obtained by using N_2-BET adsorption data and mathematical models, however, suggested that a single theoretical approach could not provide complete information about the surface structure of the produced activated carbons. It

was also shown that the α_s method provides a better estimate of the total micropore volume for highly activated carbons with wide pore size distribution. The calculated DR micropore volumes for activated carbons and the microporous structure were in good agreement with those obtained with the α_s method, while estimated micropore volumes from the α_s method deviated markedly from those obtained with the DR equation for carbons with predominantly mesoporous structures.

The SANS studies have shown that the microscopic structure of the activated carbons produced from paper mill sludge is strongly dependent on the ratio of $ZnCl_2$ used in their preparation. The scattering data from the powder samples showed that the carbon samples contain tubular pores whose radii increased with increasing amount of $ZnCl_2$ used in the preparation. The average size of the scattering objects (pores) also increased with the $ZnCl_2$ concentration. The contrast variation SANS study clearly shows that the carbon samples consist primarily of bulk amorphous carbon but contain particles of a Zn-rich phase, with a scattering length density of approximately 3.8×10^{10} cm^{-2}, in large voids linked by long, narrow channels. As the amount of $ZnCl_2$ used to prepare the carbons increases, within the range studied, so does the size of the Zn-rich phase particles and the length and radius of the pores linking the voids. Also, both the pore structure and the Zn-rich phase seem to be almost fully accessible to toluene. These results have helped to develop the model for the microstructure of the carbons shown schematically in Figure 10. These carbons contain two phases other than the bulk carbon: large particles of a Zn-rich phase with a scattering length density of around 3.8×10^{10} cm^{-2} located in voids and long, roughly cylindrical pores. Both the pores and the surfaces of the zinc-rich phase are accessible to the solvent.

It is important to note that for rodlike pores, the slope of log I vs log Q should be -1 over some Q range. As shown in Figure 5, a slope of -1 can be identified from 0.03 to 0.1 Å^{-1} for the $ZnCl_2$/sludge ratio of 1. This feature, however, seems to disappear as the ratio increases. The change in the curve structure(s) suggests that pores become less rodlike as the amount of zinc chloride, used for the production of activated carbon, increases. The reason for this can be seen from data presented in Table 2. As shown, the cross-sectional radius changes from 7.74 to 20.52 Å as the $ZnCl_2$/sludge ratio increases from 1:1 to 2.5:1, shifting the upper limit of the power law -1 scattering region to progressively lower values of Q.

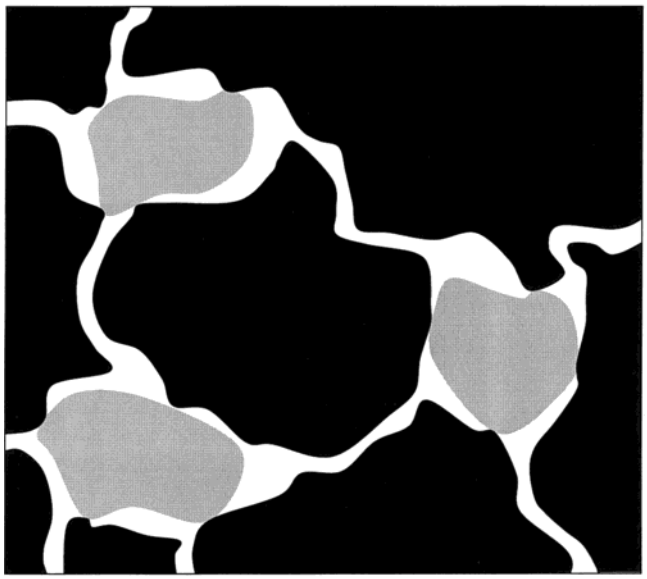

Figure 10. Schematic of the microstructure of activated carbons prepared from the paper mill sludge by using $ZnCl_2$. These carbons contain two phases other than the bulk carbon shown in black: large particles of a Zn-rich phase, with a scattering length density of around 3.8×10^{10} cm^{-2} shown in gray, and long, roughly cylindrical pores shown in white. Both the pores and the surfaces of the zinc-rich phase are accessible to the solvent.

The small pore structure of these carbons suggests that they can be used in a variety of gas phase cleaning applications. Further studies of the catalytic and adsorbate properties of these activated carbons and others similar to them when correlated with these studies of their microstructure and mesoscopic surface will allow for the preparation methods to be systematically tailored to produce activated carbons that are optimized for performance in a variety of applications.

Acknowledgment. This work has benefited from the use of the Intense Pulse Neutron Source at Argonne National Laboratory and was performed under the auspices of the U.S. Department of Energy, Office of Basic Energy Sciences, Division of Chemical Sciences under Contract No. W-31-109-ENG-38. The authors thank Denis Wozniak for his valuable assistance.

CM010653U